FINITE ELEMENT IMPLEMENTATION OF VISCOPLASTIC MODELS

V.K. Arya*
NASA Lewis Research Center
Cleveland, Ohio

The need for an accurate and realistic description of inelastic, high-temperature behavior of materials has attracted the attention of numerous investigators in recent years. As a result of their concerted efforts, a number of constitutive models called viscoplastic models has emerged. These models consider all the inelastic strain (including creep, relaxation, etc.) as a unified quantity and, in general, provide a better description of high-temperature inelastic behavior of materials. Since these models incorporate as much material science as possible, their mathematical structure is very complex. To use these models effectively and reliably for the analysis and design of turbine engine hot section components, we must demonstrate their feasibility by incorporating the models in nonlinear finite element structural analysis codes and perform nonlinear stress/life analyses for these components.

With this objective in mind, the NASA Lewis Research Center has mounted an in-house effort to implement some of the more commonly used viscoplastic models into the general purpose finite element structural analysis code - MARC. The intent is to provide the designer and structural analyst with a tool for realistic and rational analysis and designs of hot section components.

This paper gives a brief description of the implementation in MARC of two viscoplastic models developed by Robinson (refs. 1 and 2). One model is for isotropic materials and the other for metal matrix composites. Also presented are analytical results obtained for hot section components using these models. Future work is also discussed.

VISCOPLASTIC MODELS

Robinson's models for isotropic materials and metal matrix composites are based on the concept of a flow potential. The flow and growth laws for the internal variables are derived from this flow potential. The material behavior is elastic for all the stress states within the potential, and it is viscoplastic for all the stress states outside the flow potential. The displacements (strains) are assumed to be small, and the total strain is assumed to be the sum of elastic and inelastic components. The models include two internal state variables to account for the kinematic and isotropic hardenings.

A brief description of the constitutive equations of these two models and the values of constants utilized in the numerical computations are given below.

---

*NASA-NRC Resident Research Associate.

Isotropic Model

The constitutive equations for the isotropic model developed by Robinson (ref. 1) are

Flow law. -

$$2\bar{\mu}\dot{\varepsilon}_{ij} = \begin{cases} \dfrac{F^n}{\sqrt{J_2}}\,\Sigma_{ij} ; & F > 0 \quad \text{and} \quad S_{ij}\Sigma_{ij} > 0 \\ 0 ; & F \leq 0 \quad \text{or} \quad F > 0 \quad \text{and} \quad S_{ij}\Sigma_{ij} \leq 0. \end{cases}$$

Evolution law. -

$$\dot{\alpha}_{ij} = \begin{cases} 2\mu h\dot{\varepsilon}_{ij} - r\dfrac{\alpha_{ij}}{\sqrt{I_2}} ; & G > G_0 \quad \text{and} \quad S_{ij}\alpha_{ij} > 0 \\ 2\mu h_0\dot{\varepsilon}_{ij} - r_0\dfrac{\alpha_{ij}}{\sqrt{I_2}} ; & G > G_0 \quad \text{and} \quad S_{ij}\alpha_{ij} \leq 0. \end{cases}$$

where

$$S_{ij} = \sigma_{ij} - \frac{1}{3} S_{kk}\,\delta_{ij} \qquad h_0 = \frac{H}{G_0^{\beta}}$$

$$\Sigma ij = S_{ij} - \alpha_{ij} \qquad F = \left(\frac{J_2}{\kappa^2}\right) - 1$$

$$J_2 = \frac{1}{2}\,\Sigma_{ij}\Sigma_{ji} \qquad G = \sqrt{I_2}/\kappa^2$$

$$I_2 = \frac{1}{2}\,\alpha_{ij}\alpha_{ij} \qquad r = RG^{m-\beta}$$

$$h = \frac{H}{G^{\beta}} \qquad r_0 = RG_0^{\,m-\beta}$$

In the above equations, σ_{ij} denotes the stress, $\dot{\varepsilon}_{ij}$ the inelastic strain rate, δ_{ij} the Kronecker delta, and Σij the effective stress. Repeated subscripts imply summation. κ is the drag stress and α_{ij} is the back stress.

Numerical values of constants. - The values of constants are for 2-1/4Cr-1Mo steel.

$\mu = 3.61\text{x}10^7$ $\qquad \bar{\mu} = \mu \exp(\Theta_1)$

$n = 4$ $\qquad m = 7.73$

$\beta = 1.5$ $\quad R = 9.0\text{x}10^{-8} \exp(\theta_2)$

$H = 1.37\text{x}10^{-4}$ $\quad G_0 = 0.14$

and

$$\theta_1 = (23.8\theta - 2635)\left(\frac{1}{811} - \frac{1}{\theta}\right)$$

$$\theta_2 = 40\ 000\left(\frac{1}{811} - \frac{1}{\theta}\right)$$

Here, θ is the absolute temperature in degrees Kelvin.

Metal Matrix Composite Model

The constitutive equations for this model, taken from reference 2, are summarized as follows:

Flow law. -

$$\dot{\varepsilon}_{ij} = \frac{F^n}{2\mu}\,\Gamma_{ij} ,$$

Evolution law. -

$$\dot{\alpha}_{ij} = \frac{H}{G^\beta}\,\dot{\varepsilon}_{ij} - RG^{m-\beta}\Pi_{ij} ;$$

where

$$\Gamma_{ij} = \Sigma_{ij} - \xi[d_k d_i \Sigma_{jk} + d_j d_k \Sigma_{ki} - 4I_3 d_i d_j] - 4\zeta I_3(3d_i d_j - \delta_{ij})$$

$$\Pi_{ij} = \alpha_{ij} - \xi[d_k d_i \alpha_{jk} + d_j d_k \alpha_{ki} - 4I_3' d_i d_j] - 4\zeta I_3'(3d_i d_j - \delta_{ij})$$

$$F = \frac{1}{K_t^2}\left[I_1 - \xi I_2 - 12\zeta I_3^2\right] - 1 \qquad G = \frac{1}{K_t^2}\left[I_1' - \xi I_2' - 12\zeta I_3'^2\right]$$

$$I_1 = \frac{1}{2}\,\Sigma_{ij}\Sigma_{ij} \qquad I_1' = \frac{1}{2}\,\alpha_{ij}\alpha_{ij}$$

$$I_2 = d_i d_j \Sigma_{jk}\Sigma_{ki} - 4I_3^2 \qquad I_2' = d_i d_j \alpha_{jk}\alpha_{ki} - 4I_3'^2$$

$$I_3 = \frac{1}{2}\,d_i d_j \Sigma_{ji} \qquad I_3' = \frac{1}{2}\,d_i d_j \alpha_{ji}$$

$$\xi = \frac{\eta^2 - 1}{\eta^2} \qquad \zeta = \frac{4(\omega^2 - 1)}{4\omega^2 - 1}$$

Here, d_i denotes a unit vector along the preferred direction at a point of the material, and ω and η denote the anisotropic parameters.

Numerical values of constants. - In the absence of experimental data, the following values of the constants are assumed to carry out the numerical computations:

$\mu = 3.60 \times 10^7$ $\quad$ $n = 4$

$m = 7.73$ $\quad$ $\beta = 0.75$

$G_0 = 0.005$ $\quad$ $K_t = 0.82$

$R = 8.87 \times 10^{-8}$ $\quad$ $\omega = 7$

$\eta = 3$

IMPLEMENTATION IN MARC

The user subroutine HYPELA in the MARC code provides the user with an efficient way of implementing and integrating the general nonlinear constitutive relationships of Robinson's model. The details of this implementation may be found in reference 3.

To avoid the numerical instabilities encountered due to the "stiff" and "discontinuous" nature of constitutive equations, the use of "smoothing functions" (or "spline functions") is made. The spline functions used in the computations are defined in references 1 and 3.

RESULTS

Numerical results using the Robinson's models are depicted in figures 1 to 18. Figures 1 to 9 exhibit the results for the isotropic model, whereas figures 10 to 18 show the results for the metal matrix composite model.

Isotropic Model

The cyclic thermal and mechanical loads used to generate the uniaxial hysteresis loops are shown in figure 1. Three different strain rates for isothermal, non-isothermal in-phase, and nonisothermal out-of-phase loadings are shown in figures 2 to 4, respectively. Figure 5 shows excellent agreement between experiment and predictions, and verifies the correct finite element implementation of the model.

The results for the multiaxial problem of a thick internally pressurized cylinder are exhibited in figures 6 to 9. The analytical results shown in these figures were obtained using the expressions given in reference 3. The MARC and analytical results agree very well and establish the feasibility of performing a nonlinear structural analysis using the viscoplastic model.

Metal Matrix Composite Model

The results of uniaxial calculations using Robinson's metal matrix composite model are depicted in figures 10 to 18. These figures show the hysteresis loops, creep curves, and relaxation curves generated with the finite element implementation of the model. The implementation clearly shows all the expected characteristics (e.g., strain-rate sensitivity, creep, relaxation, etc.) and the effect of preferred orientations (anisotropy) of the composites. The experimental work to determine the values of constants in the model for a metal matrix composite material is in progress at Lewis.

CONCLUSIONS AND FUTURE WORK

The viscoplastic models for the isotropic material and metal matrix composites developed by Robinson have successfully been implemented in MARC. The results obtained (in particular using the isotropic model) support the feasibility of performing nonlinear structural analyses using these models. These models will provide for more realistic and rational designs of gas turbine engine hot section components.

The implementation of other viscoplastic models in MARC - such as (1) viscoplastic models for nickel-base superalloys, (2) viscoplastic models for single crystal alloys, and (3) viscoplastic models for metal matrix composites including damage - is in progress. The implementation of these models and their results, uniaxial and multiaxial predictions, will be reported subsequently.

REFERENCES

1. Robinson, D.N.; and Swindeman, R.W.: Unified Creep-Plasticity Constitutive Equations for 2-1/4Cr-1Mo Steel at Elevated Temperature. ORNL TM-8444, Oct. 1982.

2. Robinson, D.N.; Duffy, S.F.; and Ellis, J.R.: A Viscoplastic Constitutive Theory for Metal Matrix Composites at High Temperature. NASA CR-179530, 1986.

3. Arya, V.K.; and Kaufman, A.: Finite Element Implementation of Robinson's Unified Viscoplastic Model and Its Application to Some Uniaxial and Multiaxial Problems. NASA TM-89891, 1987.

CYCLIC THERMAL AND MECHANICAL LOADINGS USED TO GENERATE HYSTERESIS LOOPS BY FINITE ELEMENT CODE—MARC

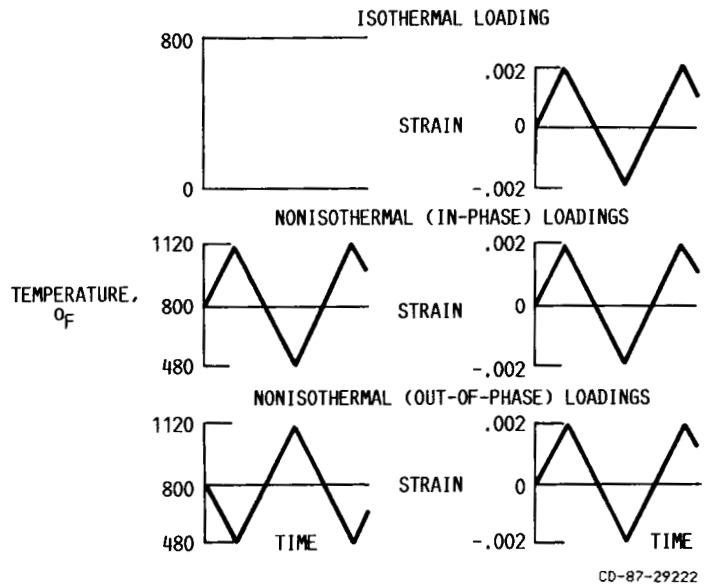

Figure 1

HYSTERESIS LOOPS AT DIFFERENT STRAIN RATES USING ROBINSON'S MODEL—ISOTHERMAL CASE, 800 °F

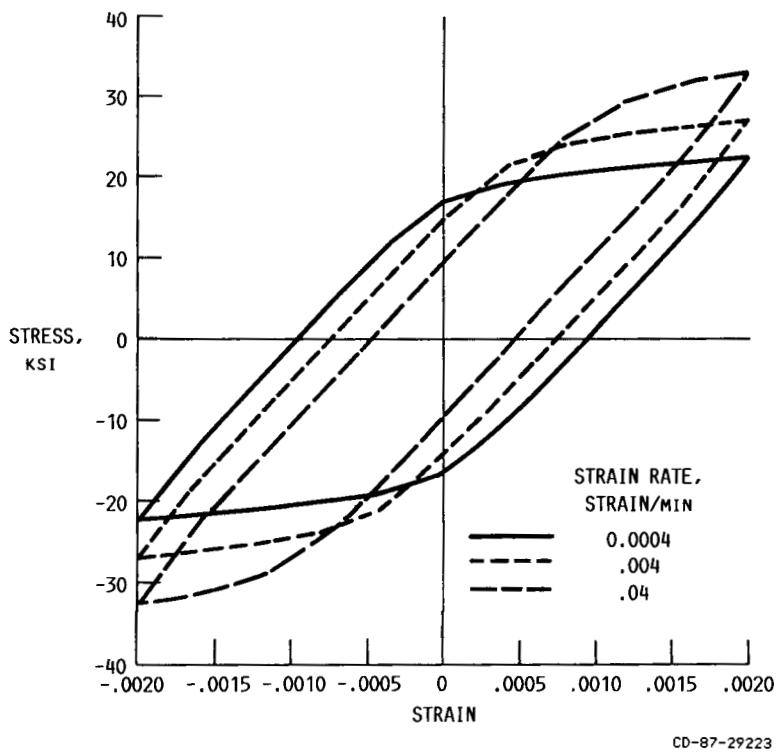

Figure 2

HYSTERESIS LOOPS AT DIFFERENT STRAIN RATES USING ROBINSON'S MODEL—NONISOTHERMAL CASE

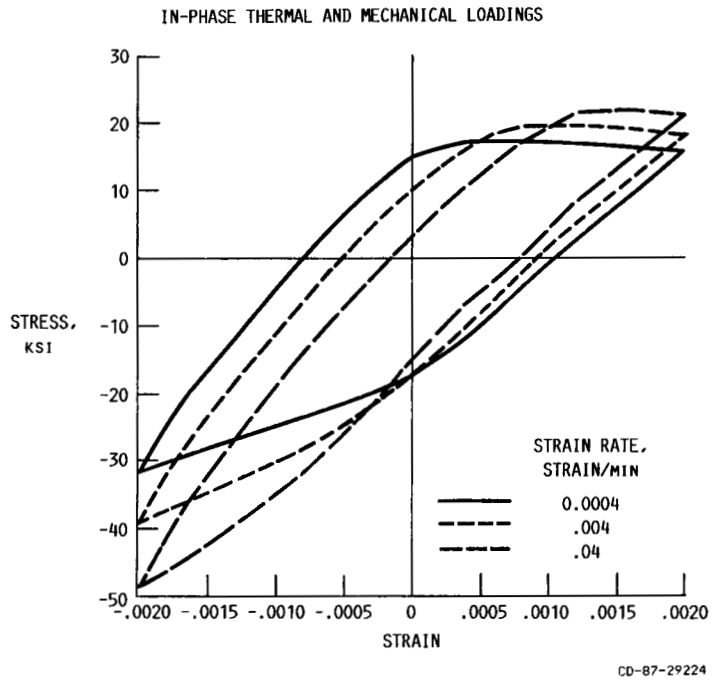

Figure 3

HYSTERESIS LOOPS AT DIFFERENT STRAIN RATES USING ROBINSON'S MODEL—NONISOTHERMAL CASE

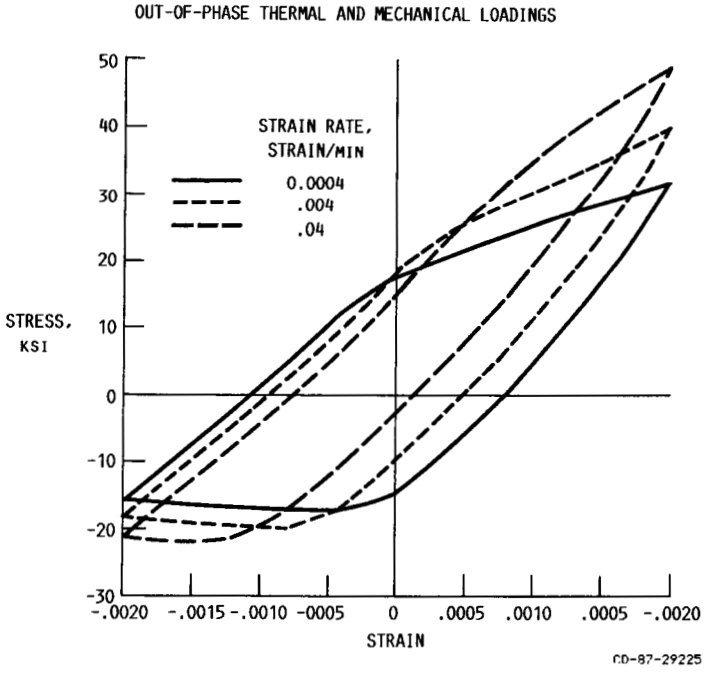

Figure 4

COMPARISON OF MARC AND EXPERIMENTAL HYSTERESIS LOOPS AT 1000 °F

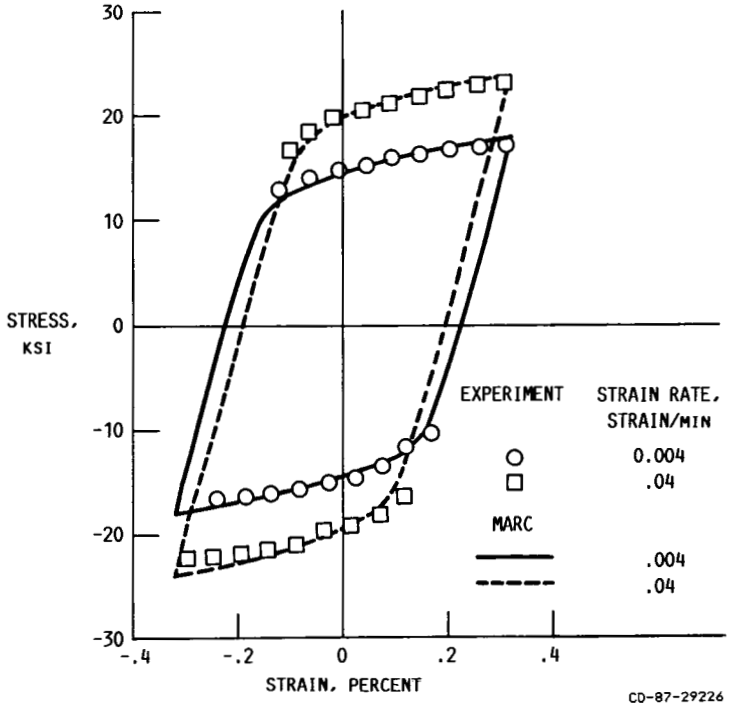

Figure 5

STRESS DISTRIBUTION IN AN INTERNALLY PRESSURIZED THICK CYLINDER USING ROBINSON'S MODEL (FEM-MARC SOLUTION)

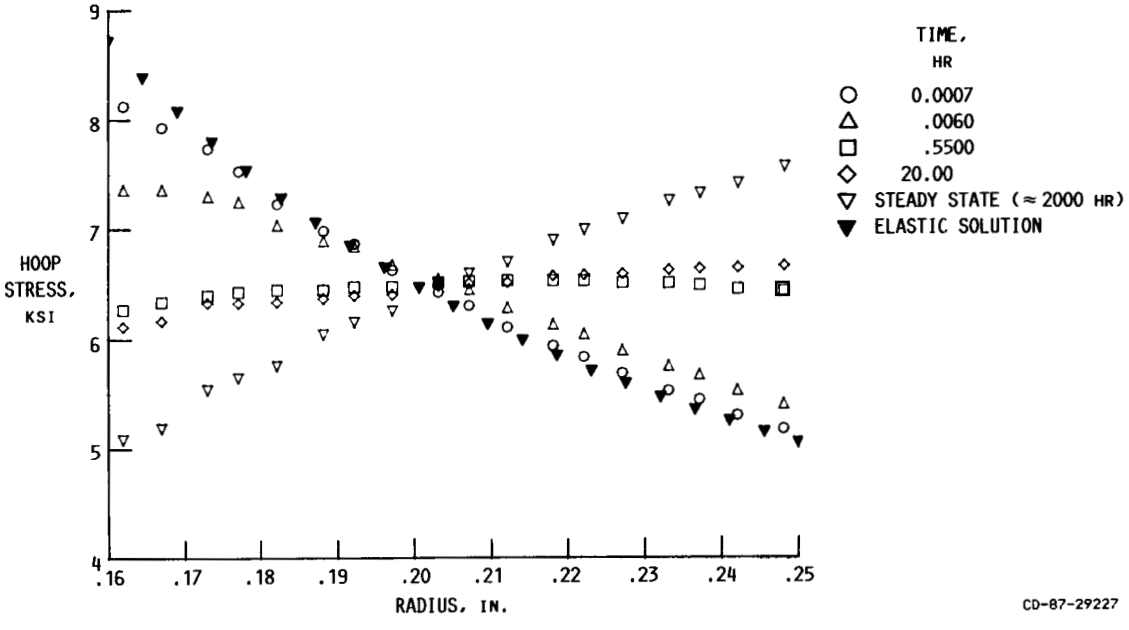

Figure 6

COMPARISON OF MARC AND ANALYTICAL RESULTS FOR STRAIN DISTRIBUTION IN AN INTERNALLY PRESSURIZED THICK CYLINDER USING ROBINSON'S MODEL

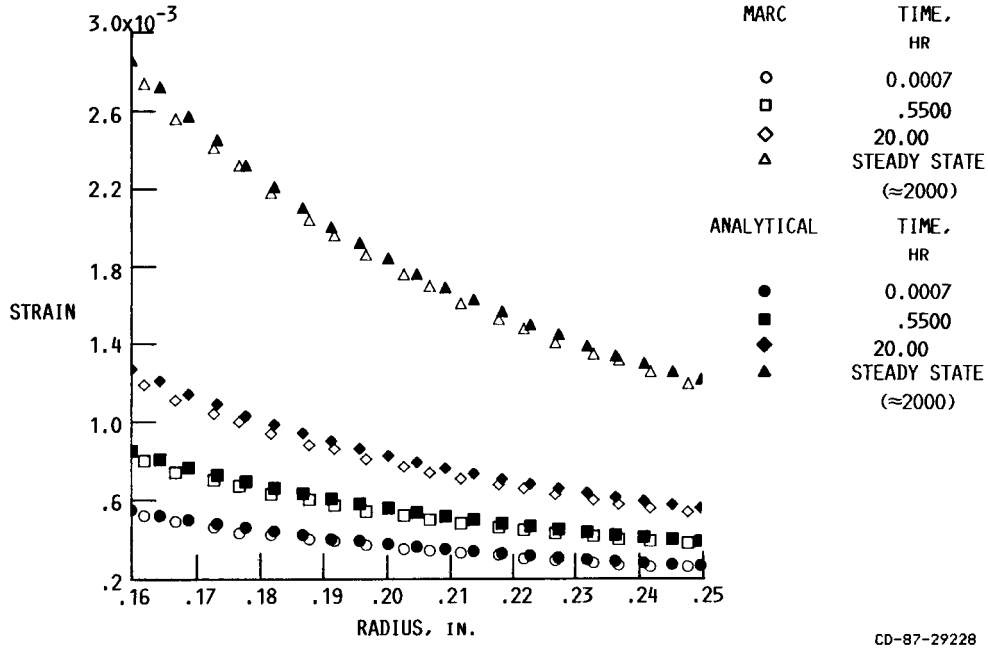

Figure 7

COMPARISON OF MARC AND ANALYTICAL RESULTS FOR STRESS DISTRIBUTION IN AN INTERNALLY PRESSURIZED THICK CYLINDER USING ROBINSON'S MODEL

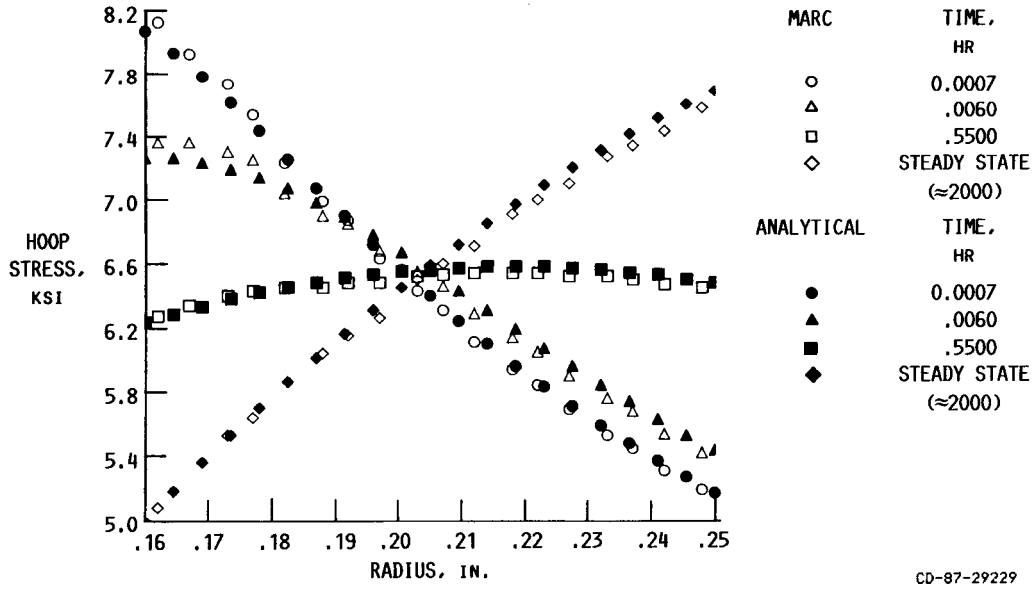

Figure 8

STRAIN DISTRIBUTION IN AN INTERNALLY PRESSURIZED THICK CYLINDER (FEM-MARC SOLUTION) USING ROBINSON'S MODEL

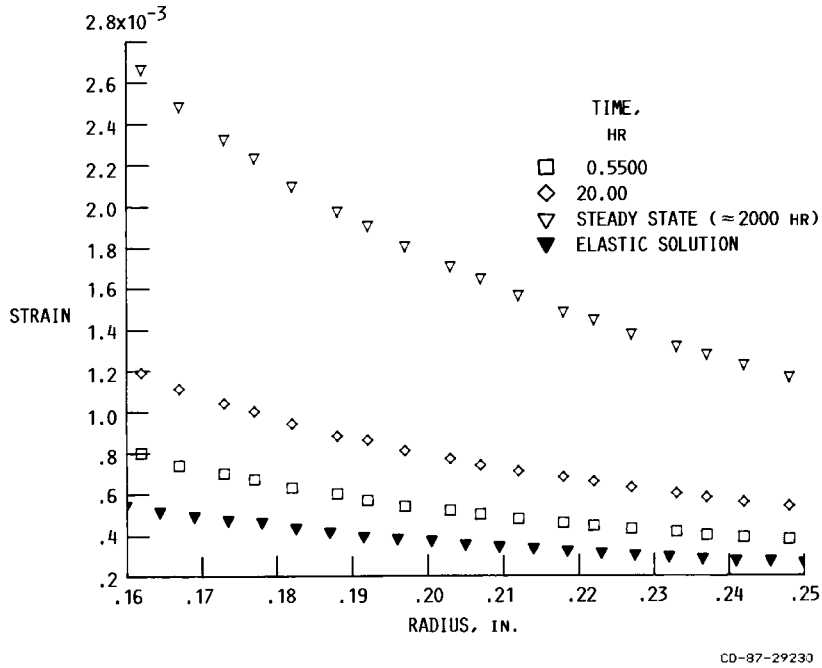

Figure 9

HYSTERESIS LOOPS AT DIFFERENT STRAIN RATES; ORIENTATION ANGLE = 0°

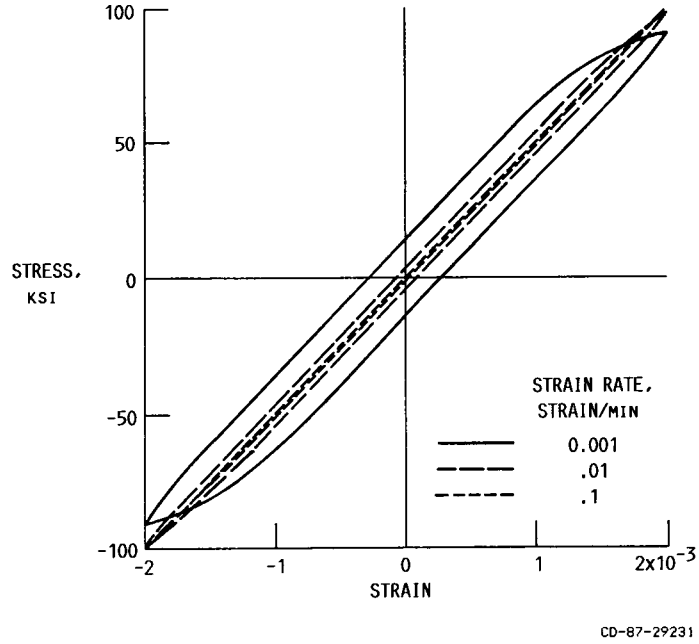

Figure 10

HYSTERESIS LOOPS AT DIFFERENT STRAIN RATES; ORIENTATION ANGLE = 30°

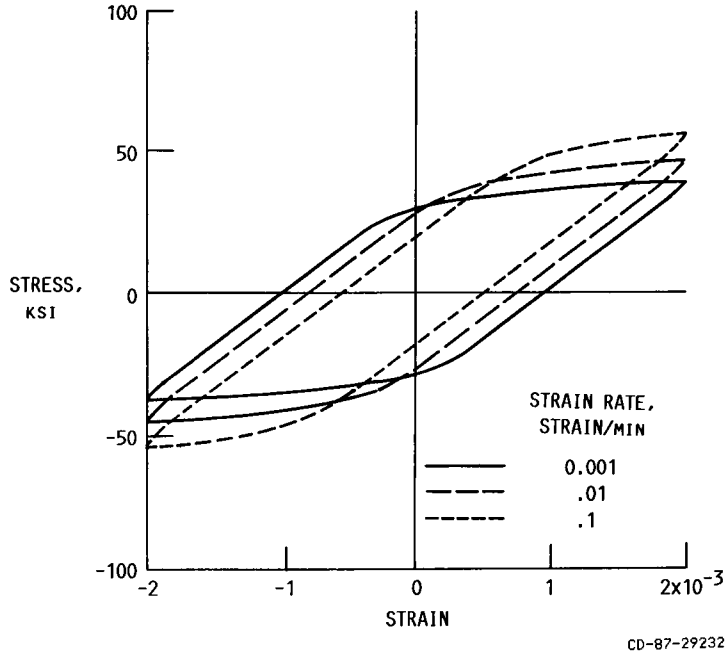

Figure 11

HYSTERESIS LOOPS AT DIFFERENT STRAIN RATES; ORIENTATION ANGLE = 60°

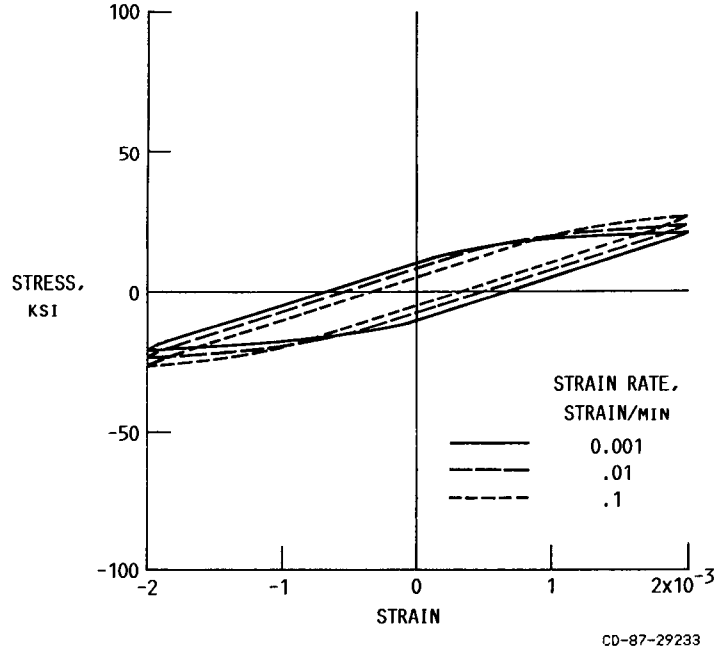

Figure 12

HYSTERESIS LOOPS AT DIFFERENT STRAIN RATES; ORIENTATION ANGLE = 90°

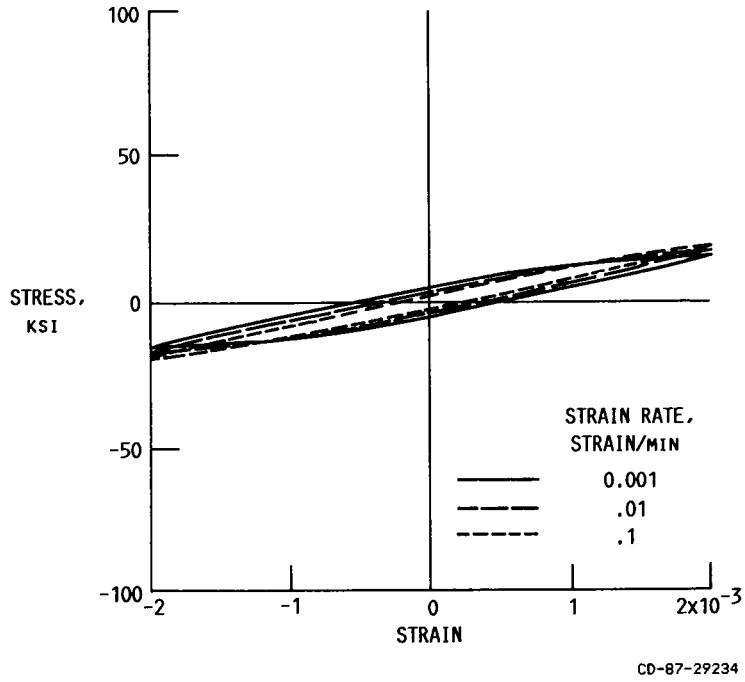

Figure 13

CREEP CURVES FOR DIFFERENT FIBER ORIENTATION ANGLES

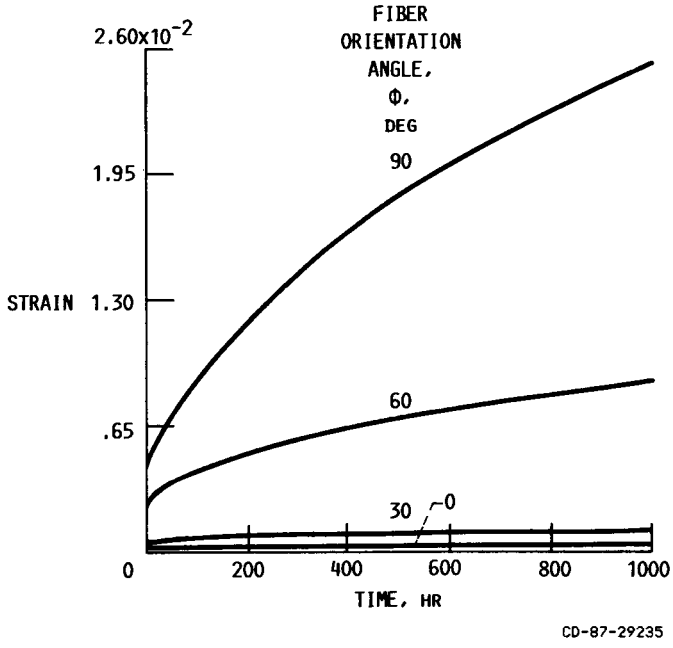

Figure 14

RELAXATION CURVES FOR DIFFERENT FIBER ORIENTATION ANGLES

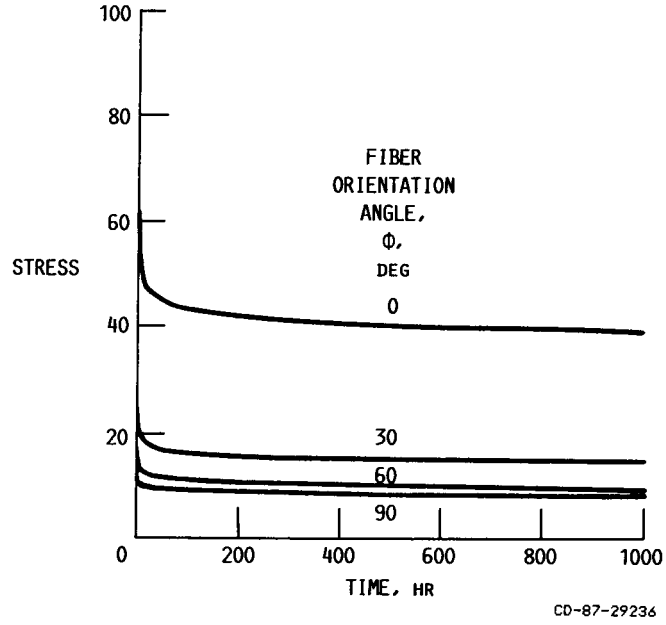

Figure 15

HYSTERESIS LOOPS FOR DIFFERENT FIBER ORIENTATION ANGLES; STRAIN RATE = 0.001/MIN

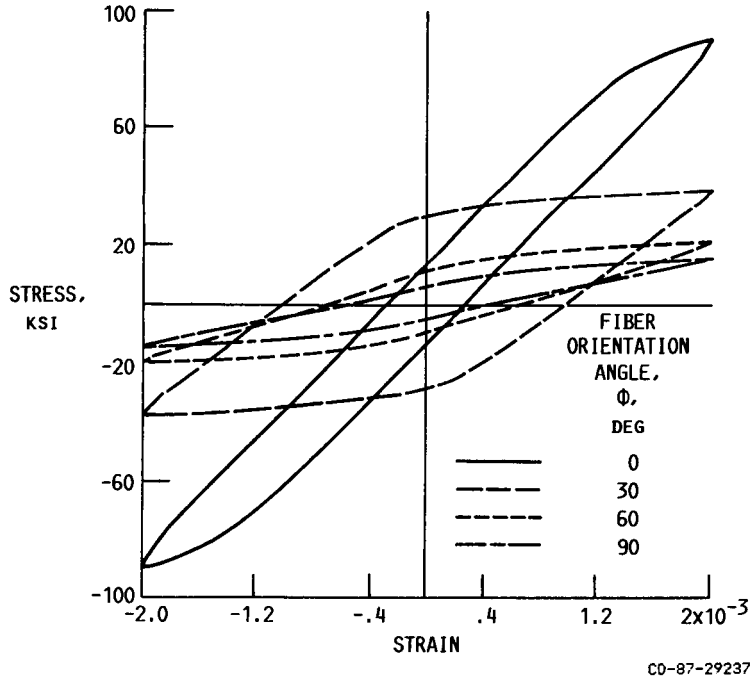

Figure 16

HYSTERESIS LOOPS FOR DIFFERENT FIBER ORIENTATION ANGLES; STRAIN RATE = 0.01/MIN

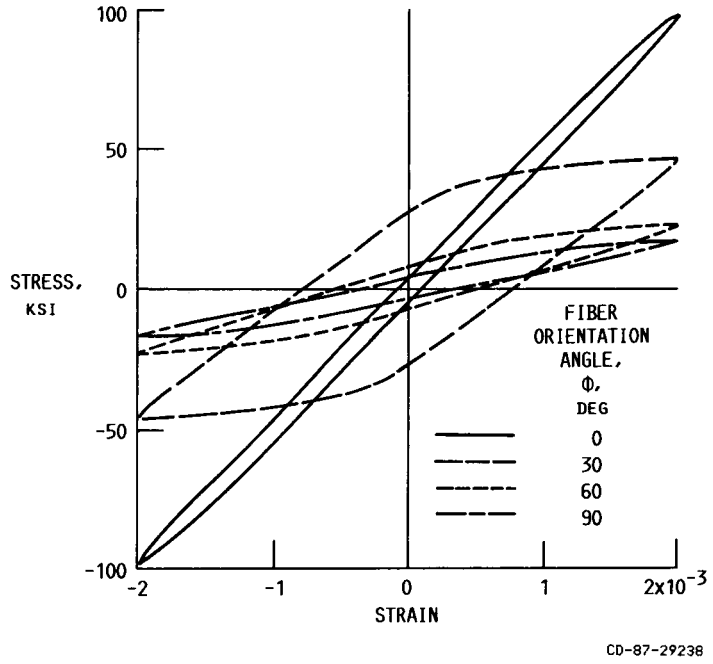

Figure 17

HYSTERESIS LOOPS FOR DIFFERENT FIBER ORIENTATION ANGLES; STRAIN RATE = 0.1/MIN

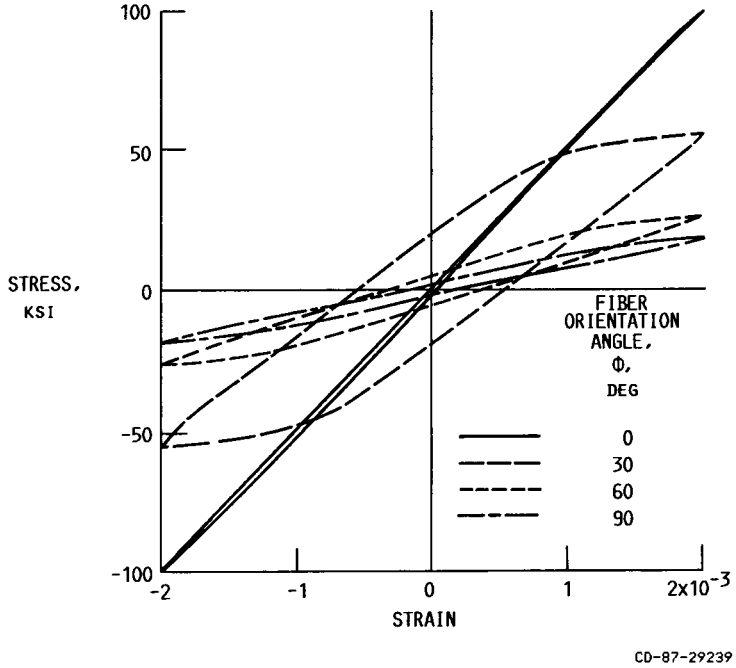

Figure 18